



An exploratory study to test sediments trapped by potholes in Bedrock Rivers as environmental indicators (NW Iberian Massif)

Un estudio exploratorio para testar los sedimentos atrapados por marmitas de erosión en ríos sobre roca como indicadores ambientales (NO Macizo Ibérico)

Álvarez-Vázquez, M.A. ⁽¹⁾; De Uña-Álvarez, E. ⁽¹⁾

(1) Department of History, Art and Geography, GEAT Research Group, Campus of Ourense, University of Vigo. As Lagoas s/n, 32004, Ourense, Spain. mianalva@uvigo.es

Abstract

The capacity of fluvial potholes to trap sediments, together with the geochemical analysis of their stored sediments for environmental assessment, is an overlooked research topic in small bedrock rivers. The present exploratory study is focused on this issue. It was developed in a small river over rock, in the inland territory of Galicia (NW Iberian Peninsula). The study started from an analysis of the inventoried fluvial potholes to identify suitable forms for sampling, and the collection of sediment samples within them. After this, the determination of the grain texture, mineralogy and content of major and trace elements in sediments were carried out. Potholes with maximum vertical depth from 25 cm to 1 m, located in central and sidewall sectors of the bedrock channel, provided the best conditions for sediment sampling. The sediments collected from six potholes showed predominance of coarse-medium grain size and sand fraction. The rough contents of the major and even trace elements are related with the nature of the more refractory minerals of the bedrock. An adequate sampling strategy, considering grain-size fractions, show potential to use trace elements as environmental indicators.

Key words: bedrock rivers; sculpted forms; sediments; major elements; trace elements; NW Spain.

Resumen

La capacidad de las marmitas fluviales para atrapar sedimentos junto con el análisis de los mismos para la evaluación ambiental es un tema de investigación poco estudiado en el caso de pequeños ríos sobre roca. El estudio exploratorio que se presenta, desarrollado en un pequeño río sobre roca del interior de Galicia (noroeste de la Península Ibérica), está centrado en esta cuestión. El estudio partió del análisis de las marmitas fluviales inventariadas con el objetivo de identificar las formas adecuadas para el muestreo y la recolección de sedimentos en su interior. A continuación, se determinó la granulometría, mineralogía y el contenido de



elementos mayoritarios y de elementos traza en los sedimentos. Las marmitas fluviales con profundidad máxima vertical desde 25 cm hasta 1 m, localizadas en el sector central y lateral del canal, presentaron las mejores condiciones para el muestreo de sedimentos. En los sedimentos recolectados en seis marmitas predomina el tamaño de grano grueso-medio y la fracción arenosa. El contenido de elementos mayoritarios y traza está relacionado con la naturaleza de los minerales más refractarios de la roca. Mediante una estrategia de muestreo adecuada, teniendo en cuenta las fracciones granulométricas, muestran potencial en el uso de los elementos traza como indicadores ambientales.

Palabras clave: ríos sobre roca; formas erosivas; sedimentos; elementos mayoritarios; elementos traza; noroeste de España.

1. Introduction

Since the mid-20th century, the increase of human activities in most fluvial systems has been modifying their natural dynamics. The impacts of industrial, urban, and recreational uses have affected their hydro-geomorphological and environmental conditions (Meybeck and Helmer, 1989; Messerli *et al.*, 2000; James and Marcus, 2006). Anthropogenic interactions with fluvial dynamics arise from changes in demographic density, land use, impoundments, and other constructed structures (Guinoiseau *et al.*, 2016; Verstraeten, 2019). One of the main human footprints in rivers is the enrichment of trace elements in water and sediments (e.g. Wilkinson *et al.*, 1997; Rice, 1999; Gaillardet *et al.*, 2003; Moatar *et al.*, 2017; Kronvang *et al.*, 2020). The research on this topic was frequently developed in floodplains, large rivers or estuaries significantly affected by human activities and with abundant fine-grained sediments (e.g. Dupré *et al.*, 1996; Vital and Stattegger, 2000; Viers *et al.*, 2009; Silva *et al.*, 2018; Uddin and Jeong, 2021). The analysis of major and trace elements in sediments from the continental realm of small rivers, headwater fluvial networks and rivers over rock is barely addressed (e.g. Grygar *et al.*, 2017; Xu *et al.*, 2017), particularly in inland areas. It causes a lack of knowledge from local reaches that set up the fluvial network in small catchments. Such an analysis can provide essential information for further sustainable use, planning and management of small fluvial systems towards the future (Biggs *et al.*, 2017) which re-

quire a research across disciplinary frontiers (Falkenmark, 1997; Wohl, 2020). Small rivers of inland Galicia (NW Spain, Fig 1A) possess suitable conditions to test the analysis of sediments in these scarcely studied watercourses. This exploratory study was developed in a small bedrock river belonging to the inland network of the Galician mainstream (the Miño River). It presents the preliminary results from a multidisciplinary research line, currently in development, considering sediments trapped by potholes. A great part of the Miño-Sil Basin (total 18,080 km²) belongs to the Galician territory (Fig. 1B). The Miño River flows along 316.63 km from its birth at Serra de Meira (Lugo, Spain, 700 m a.s.l.) to its mouth into the Atlantic Ocean, between the localities of A Guarda (Spain) and Caminha (Portugal) (CHMS, 2020). Inland Galicia the altitude increases from the medium sector of the Miño River in Ourense (Miño riverbed, 100 m a.s.l.) to the eastern mountains (Queixa, 1781 m a.s.l.; Courel-Ancares, 1969 m a.s.l.; Trevinca, 2127 m a.s.l., separated by tectonic basins). Most of Galician territory is drained by small rivers flowing over rock.

Knickpoints, stepped profiles and sculpted forms are frequent at most of the bedrock channels that combine areas of exposed rock and local alluvial veneer (Tinkler and Wohl, 1998; Wohl and Merrit, 2001). The fluvial network over rock was created by high-energy systems, providing signals of tectonic, glacioeustatic, and climatic changes connected to Earth's landscape evolution. They also generated erosive features (e.g. scallops,

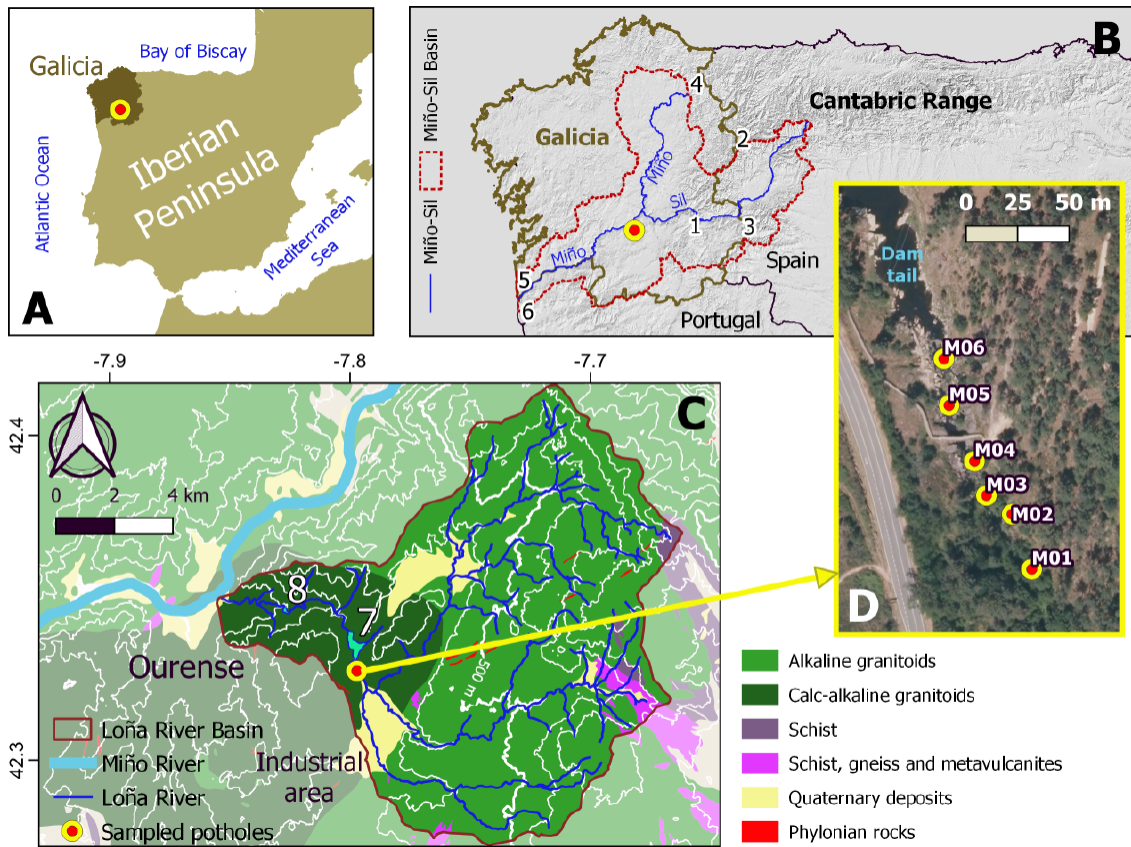


Figure 1: The Loña River in the framework of the Miño-Sil fluvial network (NW Iberian Peninsula) and location of the study site and the sampled potholes (M01 to M06). (A) Sampling site in the context of the Iberian Peninsula. (B) Sampling site in the context of the Miño-Sil basin, basemap using hillshade from EU-DEM (Copernicus), Miño-Sil course and basin from CHMS; 1 Cabeza de Manzaneda (Serra de Queixa), 2 Pico Cuiña (Serra dos Ancares), 3 Pena Trevinca (Montes de Trevinca), 4 Serra de Meira, 5 A Guarda, 6 Caminha. (C) Detail of the Loña River basin and network (CHMS) and geology settings (from ©IGME – Xunta de Galicia); 7 Cachamuíña Dam, 8 Castadón Dam. (D) Location of sampled potholes over PNOA ortophotos (©IGN). Figure made with QGIS software.

Figura 1: El río Loña en el marco de la red fluvial Miño-Sil (NO Península Ibérica) y localización del sitio de estudio y de las marmitas de erosión muestreadas (de la M01 a la M06). (A) Sitio de muestreo en el contexto de la Península Ibérica. (B) sitio de muestreo en el contexto de la cuenca del Miño-Sil, mapa base utilizando el mapa de sombras del EU-DEM (Copernicus), el curso y la cuenca del Miño-Sil de la CHMS; 1 Cabeza de Manzaneda (Serra de Queixa), 2 Pico Cuiña (Serra dos Ancares), 3 Pena Trevinca (Montes de Trevinca), 4 Serra de Meira, 5 A Guarda, 6 Caminha. (C) Detalle de la cuenca del río Loña, su red fluvial (CHMS) y la geología (©IGME – Xunta de Galicia); 7 presa de Cachamuíña, presa de Castadón. (D) localización de las marmitas muestreadas sobre ortofoto PNOA (©IGN). Figura realizada con el software QGIS.

flutes or potholes) associated to specific sedimentological patterns instream geomorphic units (Fryirs and Brierley, 2012). In bedrock channels, the magnitude of erosion, transport, and deposition processes depends on interacting feedback loops. Following Whipple *et al.* (2010), substrate lithology, together with rock fractures, joints or bedding planes, control the dominant erosion processes (i.e.

plucking and abrasion). These processes act in concert to bedload motion by fluctuations of flowing water. Hodge *et al.* (2011) point out that sediment availability result of interacting waves of discharge, motion, and deposition, interwoven with upstream and instream erosion processes. The location of sediments is determined by local channel morphology and flow hydraulics (as bedrock ribs or pot-

holes that affect flow velocities, controlling sediment storage). In addition, the definition of bedrock river segments as “governors of erosion within a river network” (Wohl, 2015: 200) is based on the idea that sediment inputs (and storage) is less than capacity of sediment transport; these conditions may be altered by dams, or other constructed human structures which influence the storage of sediments. Turowski (2020) asserts that many bedrock channels present a persistent alluvial cover, and both sediments and large blocks (from sidewalls plucking) can remain into the channel for a long time. On a reach scale (tens of meters) the position of those blocks, boulders, bedrock ribs, rock cavities and runnels regulate areas of circulating or retained water and sediments. The position and morphology of the potholes in a bedrock reach influence the movement and the accumulation of pebbles, gravel, sand or other material particles. The mobilisation of this storage during oscillations of water levels depends also on the position and morphometry of the potholes, and the arrangement of material inside these rock cavities; for example, boulders or pebbles can avoid the removal of sediments trapped below them.

Potholes are the most representative sculpted forms in bedrock channels, defined as the end-members of erosive processes from hundreds to thousands of years (Richardson and Carling, 2005; Ortega Becerril and Durán Valsero, 2010). Potholes have been studied since the 19th century (Geikie, 1865; Brunhes, 1899) regarding the erosive action of water, the variability of turbulent flows, and the evolution of rivers. Elston (1917a and 1917b) described these forms as circular or elliptical cavities, usually filled by pebbles, gravel and sand. Alexander (1932) remarked that they “constitute most efficient means for the deepening of channels in resistant rock” and distinguished morphological types by the action of different whirlpools. Some studies pointed the idea of potholes as inherited forms (Wentworth, 1944; Ives, 1948). Since 1950s, many kinds of potholes were defined, all them considering the relationships of these forms

with the channel erosion processes, their dimensional ranges and their geomorphological features (e.g. Tschang, 1957; Nemeč et al., 1982; Lorenc *et al.*, 1994; Springer *et al.*, 2006; De Uña-Álvarez *et al.*, 2009). The most recent studies emphasize the role of regional tectonics, substrate discontinuities, channel micro-topography, and flow regime in the initiation and evolution of potholes (e.g. Ortega *et al.*, 2014; Ortega-Becerril *et al.*, 2017; Álvarez-Vázquez and De Uña-Álvarez, 2017; Kanhaiya *et al.*, 2019). Nevertheless, the potential of potholes to trap sediments together with the geochemical analysis of those sediments, as it is presented by this exploratory study, has never been addressed in small bedrock rivers.

Grinding stones episodically stored into potholes are described by Das (2018) on the Subarnarekha riverbed (Jharkhand, India), analysing their role in the growth of the cavities. Ji *et al.* (2019) describe potholes that retain pebbles and cobbles in the Xunxi River (Chongqing, China), presenting a brief granulometric analysis of the particles entrapped to relate them with the growth of the cavities. In the riverbed of the Mekong River (Thailand), Udonsak *et al.* (2021) define multiple pothole types, addressing the action of pebbles and gravel for the enlargement of the cavities. This exploratory study considers the characterization of potholes as sediment traps and the analysis of the trapped sediments in the Loña River (belonging to the Miño-Sil network in Galicia). It should be noted that for rivers prevails the analysis of the suspended particulate matter (SPM), instead of sediments (e.g. Dumas *et al.*, 2015). But this approach presents some drawbacks, namely: (i) the study of SPM requires a high frequency of analysis, at least monthly/weekly (Håkanson, 2006; Håkanson *et al.*, 2005); (ii) the established SPM concentration in Galician small rivers is low (0.2-10.7 mg L⁻¹) and presents a seasonal variability of 1-2 orders of magnitude (Álvarez-Vázquez *et al.*, 2016); and (iii) the study of SPM restricts the techniques to those that require digestion of the samples, e.g. Atomic Absorption Spectrometry.

try —AAS—, or/and Inductively Coupled Plasma —ICP— (e.g. Helios Rybicka *et al.*, 2005). Consequently, the development of a suitable methodology is a need to be resolved. It must allow the aforementioned analytical techniques and others, like the increasing application of variations of X-Ray Fluorescence (XRF, e.g. Álvarez-Vázquez *et al.*, 2014; Elznicová *et al.*, 2019; Álvarez-Iglesias *et al.*, 2020). In this way, a research question was proposed: Are sediments trapped by fluvial potholes suitable to be used as environmental indicators in small bedrock rivers? Regarding this question as well as the aforementioned considerations, the research objectives were to obtain site-specific data for small rivers over rock; to describe the morphological features of potholes with capacity to trap sediments; and to explore the meaning of sediment composition in the sediments trapped by potholes.

2. Study site

The geological and geomorphological setting of the NW Spain were mainly originated during the post-Hercynian and Cainozoic times, when older tectonic structures were reactivated (Martín-González, 2009). This process caused the tectonic deformation of Precambrian and Paleozoic rocks. According to Vegas (2010), the configuration of the relief of Galician follows a general direction NNE-SSW, being the western continuation of the Cantabrian Range (Fig. 1B). Its central area, the Galician Massif, connect to the North of Portugal through the Corridor of Ourense, delimited by faults and strongly incised by the fluvial network of the Miño River. The morphology of the Galician Massif is characterized by deep fluvial valleys following the tectonic structures and Hercynian granitic bodies exposed at different heights Vidal-Romaní *et al.*, 2005; Vidal-Romaní *et al.*, 2014). Because of the tectonic deformations, the current configuration of the Miño-Sil fluvial network started from the change of the Sil flow (from eastwards to westwards) and its capture by the headward erosion of the older Miño; likewise, a differential uplifting process

generated the current relief configuration that alternate mountain blocks and depressions. The presence of stepped erosive or etch surfaces and multiple terrace levels (Viveen *et al.*, 2012 and 2014) prompt uplift until Quaternary times.

The Loña River (19.96 km long) is a small tributary of the Miño River in the inland Galicia (Fig. 1C), draining a basin of 139 km² that includes two distinct sectors: in the first, from its birth to the locality of Cachamuiña (Ourense), the river flows towards the SSW over an etched surface (average altitude of 400 m a.s.l.) (Yepes Temiño, 2002) with a gentle slope (3%); in the second, the river flows towards the WNW through a deeply incised valley (slope of 9%) until its confluence with the Miño River in the town of Ourense (100 m a.s.l.). The basement is constituted by granitic rocks emplaced into Palaeozoic meta-sediments during the Hercynian orogeny, including calc-alkaline types (granodiorites that belong to the Ourense Massif) and alkaline types (two mica granites, leucogranites) (Capdevila and Floor, 1970). In this hydrographic unit, climate presents temperate sub-humid conditions with a short dry period in summer (De Uña-Álvarez, 2001); the average for annual temperature is 11.3 °C and the annual total precipitation and evapotranspiration values are 1,376 mm and 490 mm respectively (CHMS, 2020). The amount of the annual hydrological resources from the Loña system (2,990 hm³, average annual flow in natural conditions of 2.08 m³ s⁻¹) is currently regulated by two dams. The reservoirs were constructed in the aforementioned second sector, to wit, the Castadón dam (1929, capacity of 0.2 hm³) and the Cachamuiña dam (1954, capacity of 1.8 hm³); both are devoted to urban water supply. The minimum ecological flow ranges from 0,140 m³·s⁻¹ (October - December) to 0,541 m³·s⁻¹ (April - June).

The study site is a fluvial reach (central point: 42° 19' 39" N; 7° 47' 59" W) located just upstream of the Cachamuiña dam (Fig. 1C and 1D), with a length of 300 m and increasing width downstream from 9 m to 56



Figure 2: Views of the study site, showing the limits of the fluvial reach from the west (A), and from the east (B). Main types of identified potholes: C) small saucer-shaped pothole; D) central pothole with asymmetrical cross-section; E) lateral potholes with several erosive levels; and F) Big pothole developed in the sidewall of the bedrock channel.

Figura 2: Vistas del sitio de estudio, mostrando los límites del tramo fluvial desde el oeste (A) y desde el este (B). Principales tipos de marmitas identificados: C) pequeña marmita con morfología en platillo; D) marmita central con sección transversal asimétrica; E) marmitas laterales con varios niveles erosivos; y F) Gran marmita desarrollada en la pared lateral del canal sobre roca.

m. The basement of the reach is constituted by coarse-grained granodiorites; upstream the reach, the fluvial network flows mainly over two mica granites and leucogranites (fine-medium grained) and small schist areas; in addition, sedimentary deposits generated by weathering (boulders, sands and clays)

named as “non-differentiated Quaternary deposits”, cover the contact between granites (Barrera Morate *et al.*, 1989). Small hills, castle-kopjés, and tors, are characteristic landforms of the landscape that surrounds the reach. The fluvial reach is plenty of sculpted forms, mainly potholes. Following the gener-

al typology of Richardson and Carling (2005) small saucer-shaped forms (scarcely deep, rounded and with symmetrical cross-section, Fig. 2C), central potholes (more deep, asymmetrical in the plane and profile, Fig. 2D) and lateral potholes (deepest, with at least two erosive levels in the profile and basal knolls, Fig. 2E and 2F) were identified. The biggest cavities are sidewall and coalescent potholes developed in the walls of the channel, where rock blocks limited by open discontinuities are removed during high flows. Potholes located in central and lateral areas of the bedrock channel preserve a part of their walls.

According to the EU Water Framework Directive, the Loña is a small Cantabrian-Atlantic Siliceous River of the Iberian-Macaronesia eco-region (CEDEX, 2004), defined as a water mass with a good level of water chemical conditions and a moderate level of water ecological conditions (CHMS, 2020). This last is related to punctual sewerage spills as well as the effects of the dams (e.g. nutrients provided by wastewater, together with the impounded water within the dam, can lead to eutrophication phenomena).

3. Methodology

The complete report of all sculpted forms present in the bedrock channel of the Loña River was carried out during 2012, ending the previous prospections. This fieldwork was the departure point to define the potential of potholes as sediment-traps. A detailed inventory of 62 cases was created from 2012 to 2014, followed by the study of the potholes with capacity to store sediments. The dimensional and morphological analysis of the inventory provided the definition of several pothole types. The selection of the potholes that had suitable properties according to the scope of the study, started from the measures of maximum depth and opening axis, together with other qualitative features (e.g. the shape of bottom micro-relief and the morphology of the inner walls). Afterwards, sediments from six potholes (Fig. 1D) were sampled with a

plastic spatula and stored in plastic zip bags. Once in the laboratory, samples were weighed and oven dried at 45 ± 5 °C until constant weight. After that, samples were sieved through 2 mm and 0.063 mm mesh to separate the gravel (> 2mm), sandy (< 2 mm), and mud (< 0.063 mm) fractions. The various fractions (when present) were stored in plastic containers until analysis.

In order to attain the research objectives, the characterization of the samples was based on their grain texture, mineralogical composition, and concentrations of major and trace elements. Considering the grain texture of the samples, the < 2 mm fraction (sand in general terms due to the scarcity of fine particles) was selected for the determination of mineralogical composition and contents of major (i.e. Al, Ca, Fe, K, Mg, Na, and Si) and trace elements (i.e. As, Cr, Cu, Ni, Pb, and Zn). Mineralogy was determined by X-Ray Powder Diffraction (XRD), and the content of the major, minor and trace elements by X-Ray Fluorescence; both routine analysis in the Scientific and Technological Research Assistance Centre (CACTI, University of Vigo). Results of elemental composition were obtained utilizing the software Spectraplus, processed through the EVAL program and corrected by the k factor with the reference material PACS-2 (National Research Council of Canada). In the two samples with enough quantity of fine sediments (i.e. M02 and M05), some elements were also determined in the <0.063 mm fraction (i.e. Al and Fe as widely used reference elements; Cu, Pb and Zn as common contaminants related to human activities). This supplementary analysis was performed in the Laboratory of the Marine Biogeochemistry Group of the Marine Research Institute (IIM-CSIC). These analyses were conducted by Electrothermal (ETAAS) and Flame (FAAS) Atomic Absorption Spectrometry, using for quality control the aforementioned reference material PACS-2. Statistical analysis of the data was developed using the StatGraphics Centurion 18 software. An exploratory clustering gets together with the analysis of statistical correlations of the data variables.

4. Results and discussion

4.1. Potholes as sediment traps

The potholes developed in the Loña reach encompass a wide diversity of cavities whose position and morphological configuration are key factors for their potential to trap sediments. Following the classification from some Spanish bedrock rivers (Nemec *et al.*, 1982; Lorenc *et al.*, 1994; Lorenc *et al.*, 1995) the potholes of the study site include incipient forms (rounded, symmetrical cross-section) together with developed forms (elliptical or cylindrical, asymmetrical

cross-section, knolls in the bottom) and very developed forms (asymmetrical cross-section, coalescences, knolls in the bottom, and top rims). These authors indicate, as an additional feature, that potholes in incipient stages (with opening diameters from 20 to 40 cm) already contain small pebbles. As a whole ($n=62$), the maximum vertical depth (D) of the Loña potholes ranges from 6.5 cm to 4 m and the measures of their opening axis (A) ranges from 8 cm to 3 m (Fig. 3A, 3B and 3C). Many potholes recorded in the Loña reach have opening planes with hemi-ellipsoidal, hemispherical or complex geometry, bottom planes with compound concave and

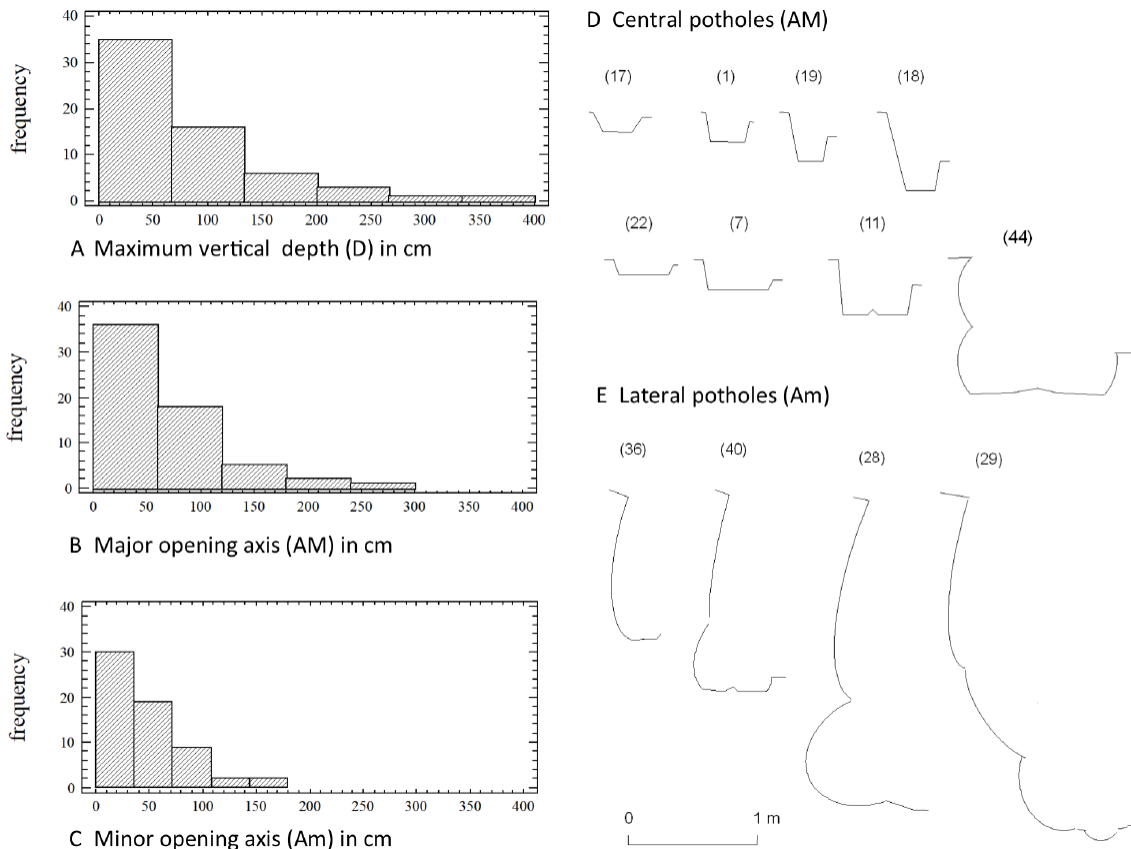


Figure 3: Features of the potholes recorded in the Loña reach ($n=62$). Histograms represent the absolute frequencies of the recorded values for the maximum vertical depth (A), the major opening axis (B) and the minor opening axis (C). Also presented the main types of profiles in the central (D) and lateral potholes (E). The numbers in brackets refer to the number of the potholes in the inventory.

Figura 3: Características de las marmitas en el tramo del Loña ($n=62$). Los histogramas representan las frecuencias absolutas de los valores registrados para la profundidad máxima vertical (A), el eje mayor de apertura (B) y el eje menor de apertura (C). También se muestran los tipos principales de la morfología de los perfiles en las marmitas centrales (D) y laterales (E); los números entre paréntesis indican el número de la marmita en el inventario.

convex micro-relief, and stepped cross-sections including multiple levels of erosive sequences (Fig. 3D and 3E). Their position in the lateral or central areas of the bedrock channel also determines the existence of submerged and semi-submerged forms. Near the study site, in the urban reach of the Miño River across the city of Ourense (Álvarez-Vázquez and De Uña-Álvarez, 2015), potholes developed in the bedrock with $D=20$ cm present asymmetrical profiles (trapping pebbles), and when D achieves 40 cm (being $A \leq D$) retain deposits of more than 10 cm of sediments (vertical thicknesses).

Alike the more developed potholes described in the Orange River (Springer *et al.*, 2006), many potholes in the selected reach have inner surfaces with sections of polished rock and only preserve a part of their walls. The configuration of the potholes in the study site is very affected by the discontinuities of the rock, appearing morphologies similar to drop, kidney, truncated, confined, multi-joint, and teardrop potholes, as formerly described in the Bedrock Rivers of the Spanish Central System (Ortega *et al.*, 2014). In the Loña reach (Fig. 4), the potholes with smaller dimensions are always located in the middle of the bed-



Figure 4: Some examples of potholes inventoried in the Loña reach. A) lateral potholes, a) big pothole with maximum vertical depth of 2.7 m and major opening axis of 1.9 m, b) compound pothole with blocks and pebbles, maximum vertical depth of 1.8 m and major opening axis of 2.0 m. B and C, the pothole b in early spring (b_1) and early summer (b_2). D) pothole covered by a block (c_1) with maximum vertical depth of 78 cm, and tube shape pothole (d_1) with maximum vertical depth of 1.2 m (early spring). E) the same potholes refer to c_2 and d_2 (early summer). F) singular pothole, with maximum vertical depth of 1.8 m and major opening axis of 1.3 m.

Figura 4: Algunos ejemplos de marmitas inventariadas en el tramo del río Loña. A) marmitas laterales, a) gran marmita con 2.7 m de profundidad máxima vertical y 1.9 m en el eje mayor de apertura, b) marmita compuesta con bloques y cantos, con 1.8 m de profundidad máxima vertical y 2.0 m en el eje mayor de apertura. B y C, la marmita b al comienzo de la primavera (b_1) y al comienzo del verano (b_2). D) marmita cubierta por un bloque (c_1) con 78 cm de profundidad máxima vertical, y marmita tubular (d_1) con 1.5 m de profundidad máxima vertical (comienzo de la primavera). E) las mismas marmitas identificadas por c_2 y d_2 (al comienzo del verano). F) marmita con forma singular, con 1,8 m de profundidad máxima vertical y 1.3 m en el eje mayor de apertura.

rock channel; these central potholes include forms with $A > D$ (maximum values for D is 25 cm) and forms with $A \geq D$ (maximum values for D is 60 cm). Other central potholes and lateral potholes (located in the walls of the channel) are forms with $A \geq D$ (maximum value for D is 1.10 m); lateral potholes frequently present an open-tube shape. The potholes with larger dimensions are always located in the walls of the bedrock channel being always compound and coalescent forms with $D > A$ (maximum value for D is 4 m); these potholes barely retain sediments or sediments are gathered below boulders and pebbles.

Biggest potholes developed in the undulated walls are opened cavities (D between 2 m and 4 m), with very scarce capacity to retain sediments. The potholes developed in lateral or central sectors of the bedrock channel (D between 26 cm and 1 m) have capacity to trap pebbles and sediments that ranges from 15 to 50 cm (vertical depth of storage). This feature makes them suitable for an exploratory study of their trapped sediments. Thus, six potholes were selected for it, considering the best conditions of the trapped particles for sampling. At the time of sampling (Fig. 5), three potholes were located above the flow level in the bank of the bedrock channel, and so, they were dry (M02, 311 m a.s.l.; M03, 315 m a.s.l.; and M05, 311 m a.s.l.); one pothole, a multi-level sculpted form in the rock walls

of the bedrock channel (M01, 310 m a.s.l.), was partially submerged; and two potholes, in the low-central sector of the bedrock channel (M04, 310 m a.s.l., and M06, 329 m a.s.l.), were flooded.

4.2. Analysis of trapped sediments

The grain texture of the sediments is dominated by sands (average $\approx 60\%$) and gravels (average $\approx 40\%$); the fine fraction (< 0.063 mm) was very scarce, in average a 0.4% of dry weight. This textural distribution (Fig. 5) is frequent in bedrock channels, accumulating coarse sediments from sand size upwards. According to Tinkler and Wohl (1998). This coarse sediment accumulation is caused by high-energy systems where the capacity of the channel to trap sediments is typically restricted to rock cavities. The mineralogical composition of the sandy fraction (< 2 mm) is dominated by silica (74-84%); the proportion of feldspars (microcline, 9-12%, and albite, 5-10%) accounted from 14 to 22%, and the results also show a lesser proportion of micaceous minerals (muscovite, 2-3%). This mineralogical composition is reflecting the igneous origin of the sediments from the granites and granodiorites of the basin (Capdevila and Floor, 1970; Barrera Morate *et al.*, 1989). The parental rock also seems to represent the driver determining the abundance of major

Table 1: Composition of major elements in the sediments, compared with references. Data provided in %.

Tabla 1: Composición de los elementos mayoritarios en los sedimentos. Datos expresados en %.

Element	Loña Min-(Median)-Max	Local rocks ^(a)	UCC ^(b)
Al	4.3-(4.9)-6.2	7.1-7.7	8.2
Ca	0.07-(0.10)-0.12	0.29-0.66	2.6
Fe	0.33-(0.39)-0.49	0.5-2.0	3.9
K	2.5-(3.0)-3.5	2.9-4.1	1.2
Mg	0.03-(0.05)-0.06	0.06-0.20	1.5
Na	0.9-(1.0)-1.3	2.2-3.1	2.4
Si	39-(41)-42	34-35	31.1

(a) Barrera Morate *et al.* (1989) composition of local granites and granodiorites.

(b) Rudnick and Gao (2003) composition of the upper continental crust.

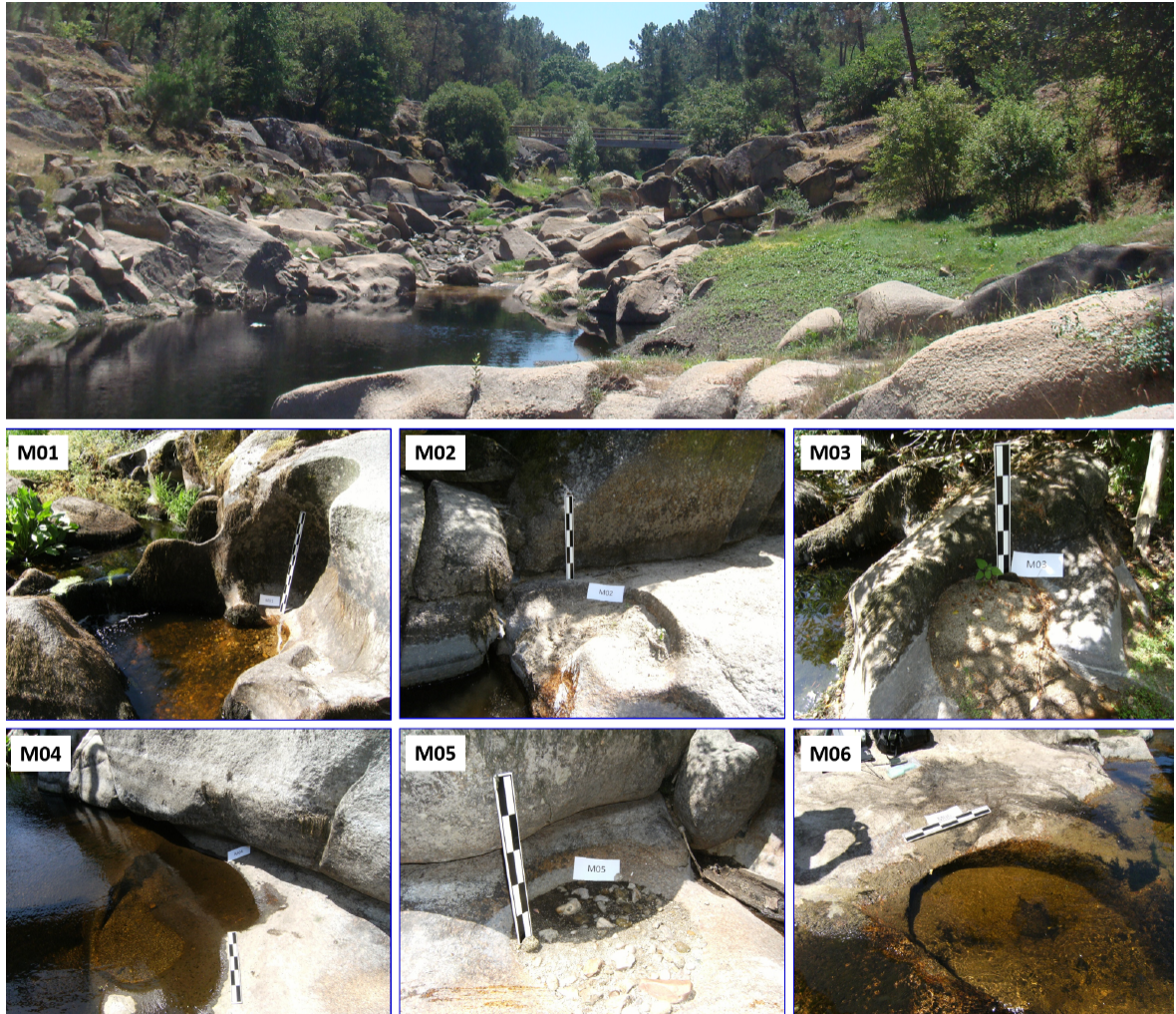


Figure 5: General view of the reach from west and images of the sampled potholes (M01 to M06) in the moment of sediment sampling (before collection).

Figura 5: Vista general del tramo desde el oeste e imágenes de las marmitas muestreadas (de la M01 a la M06) en el momento del muestreo de sedimentos (antes de la recolección).

elements in the samples: four elements accounts for around a 50% of the bulk composition, i.e. in decreasing average order, Si (41%), Al (5%), K (3%) and Na (1%). Typical major constituents are over here in the range of minor concentrations (less than about a 1% until a 0.01% of the samples), to wit: Fe (0.4%), Ca (0.1%), and Mg (0.05%). Considering that basically sand (quartz) is composing the samples under study (containing the refractory silica of the parental rock), the results presented in Table 1 show enrichment in Si and depletion in the other major constituents. The cause

might be the weathering of the less resistant minerals into fine particles, which have been transported downstream.

This linkage with the rock mineral composition is also highlighted by the cluster analysis (Fig. 7). Almost all the studied major constituents (except Si) are grouped with the potassium-rich alkali feldspar microcline (MIC). They are also related, in a lesser extent, with the plagioclase feldspar albite (ALB) and the micaceous hydrated phyllosilicate muscovite (MUS). The variation of trace elements con-

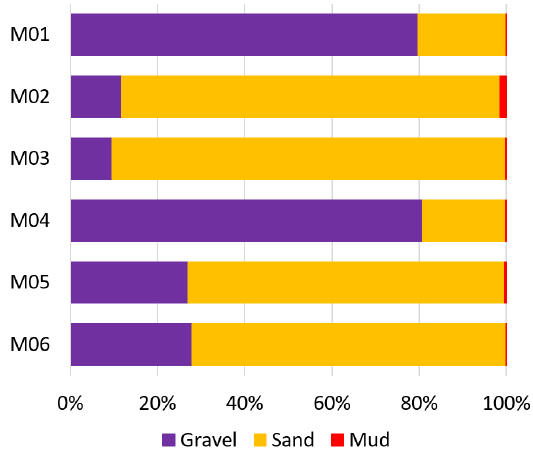


Figure 6: Grain texture of the sediments trapped by potholes. The bars indicate the relative frequency (%) of the separated fractions, i.e. gravel (> 2 mm), sand (< 2 mm and > 0.063 mm) and mud (< 0.063 mm).

Figura 6: Granulometría de los sedimentos atrapados por las marmitas de erosión. Las barras indican la frecuencia relativa (%) de las fracciones separadas, i.e. gravas (> 2 mm), arenas (entre 2 y 0.063 mm) y fangos (< 0.063 mm).

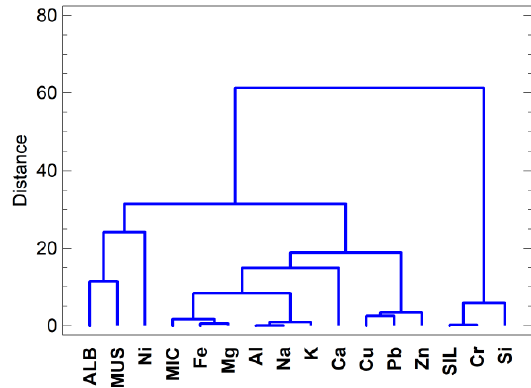


Figure 7: Dendrogram from clustering (Ward's Method, Squared Euclidean) showing the linkage between mineralogy (i.e. ALB is albite, MIC is microcline, MUS is muscovite and SIL is silica), major elements (i.e. Al, Ca, Fe, K, Mg, Na and Si) and trace elements (i.e. Cu, Cr, Ni, Pb and Zn) in the sediments (fraction < 2 mm) trapped by potholes.

Figura 7: Dendrograma resultado del análisis clúster (método de Ward, distancia euclídea al cuadrado) mostrando las relaciones entre la mineralogía (i.e. ALB es albite, MIC es microclina, MUS es moscovita y SIL es sílice), los elementos mayoritarios (i.e. Al, Ca, Fe, K, Mg, Na y Si) y los elementos traza (i.e. Cu, Cr, Ni, Pb y Zn) en los sedimentos (fracción < 2 mm) atrapados por las marmitas de erosión.

Table 2: Trace elements statistics in the Loña River potholes sediment samples, also compared with several references.

Tabla 2: Estadísticas de los elementos traza en los sedimentos atrapados en marmitas de erosión del río Loña, comparados con varias referencias.

	Cr (mg kg ⁻¹)	Cu (mg kg ⁻¹)	Ni (mg kg ⁻¹)	Pb (mg kg ⁻¹)	Zn (mg kg ⁻¹)
Average	29.3	17.5	10.6	21.9	28.9
Standard deviation	16.5	7.5	3.0	6.9	9.2
Minimum	9.8	9.5	6.6	13.6	12.1
Median	27.0	16.4	10.3	21.5	29.9
Maximum	50.6	29.0	15.1	33.3	38.3
UCC ^(a)	92	28	47	17	67
Galician sediments ^(b)	22.9	14.7	29.2	21.0	48.3
Galician estuarine sediments ^(c)	41-101	10-27	12-47	18-50	70-100
Spanish floodplain sediments ^(d)	61.6	22.6	27.9	42.5	80.7

(a) Rudnick and Gao (2003) composition of the upper continental crust.

(b) Macías Vázquez and Calvo de Anta (2009), total fraction in uncontaminated areas, average + 2SD.

(c) Álvarez-Vázquez *et al.* (2020; 2017a), muddy flats, Álvarez-Vázquez *et al.* (2014; 2018), <0.063 mm fraction, background values. (d) Locutura Rupérez *et al.* (2012), <0.063 mm fraction, background values.

tent in the <2 mm fraction of the sediments is also related to the rock mineralogy. Three groups can be differentiated in the cluster analysis (Fig. 7): (i) Cr is in a group with the refractory quartz (silica) and thus with Si. The most numerous group of variables (ii) is related with microcline, the second most abundant mineral in the samples (i.e. 9-12%). In this group, with major constituents (i.e. Al, Ca, Fe, K, Na and Mg), the trace elements (i.e. Cu, Pb and Zn) seem to be part of a subgroup. Variations are principally related to the mineralogical composition, but any hidden factor can be behind the distribution of Cu, Pb and Zn. (iii) Ni is clustered with albite and muscovite. The contents of trace elements are, in general, similar to or even below different background values (see statistics and comparison with references in Table 2).

The results from the rank correlations (Spearman coefficients with p-value < 0.05) indicated strongly direct associations for Al and Na (0.98), Al and K (0.98), Mg and Fe (0.92), P and Ca (0.92); and they were of negative sign for Si and Al (-0.94), Si and K (-0.88), Si and Na (-0.92). The analysis of the data reported that standard skewness and kurtosis, for each of the selected data variables, was within the range of -2 to +2. Testing a Pearson product moment correlation between each pair of variables only statistically significant non-zero direct correlations will be further presented (P-values below 0.05, 95% confidence level). The results are coherent with the mineral composition of the samples. In the one hand, microcline is correlated with Fe ($r = 0.84$) and

Mg ($r = 0.91$), within this group Fe also show a correlation with Na (0.83) and Mg (0.93); Mg with Al (0.87), Na (0.92) and Pb (0.90); while silica only with Cr (0.98) and muscovite and albite did not present any statistically significance correlation with the variables under study. In the other hand, there is a statistically significant linear relationship between Cu, Pb and Zn ($r > 0.82$). This correlation between these three last elements, together with the results of the cluster analysis (Fig. 7) indicate that the variation in their contents cannot be explained only by the natural variation of the mineralogy.

The fine fraction (<0.063 mm) is frequently employed in environmental assessment “to reduce the confounding effects of variable grain size and to ensure comparability of spatial and temporal data for pollutant dispersion” (Birch and Lee, 2020). To compare, the fine fraction of samples M02 and M05 was analysed by FAAS (i.e. Al and Fe) and ETAAS (i.e. Cu, Pb and Zn). Precise results are presented in Table 3. Only the two aforementioned samples provided enough quantity of fine sediments to perform the analysis (the fine fraction was 1.4% and 0.4%, respectively). Major elements (i.e. Al and Fe), presented a different behaviour. The contents of Al in the fine fraction were moderately lower but similar to those in the <2 mm fraction (in a factor of 0.9 for M02 and 0.8 for M05). Unlike, Fe is enriched in the fine fraction, in a factor of 6.0 in M02 and 2.2 in M05. The weathering of the most mobile minerals can explain the loss of Al, being exported downstream as fine

Table 3: Composition comparison between the sandy (<2 mm) and fine (< 0.063 mm) fractions of the sediments.
Tabla 3: Comparación de la composición entre las fracciones arenosa (<2 mm) y fina (< 0,063 mm) de los sedimentos.

Sample (fraction)	Al (%)	Fe (%)	Cu (mg kg ⁻¹)	Pb (mg kg ⁻¹)	Zn (mg kg ⁻¹)
M02 (<2 mm)	6.2	0.44	29.0	33.3	38.3
M02 (< 0.063 mm)	5.7	2.62	47.7	106.8	455.0
M05 (< 2 mm)	6.1	0.49	22.3	23.8	35.5
M05 (< 0.063 mm)	5.0	1.09	19.7	44.9	119.7
Ref. SPM Galician Rivers ^(a)	3.9-5.0	6.2-34.3	29-42	18-29	14-53

(a) SPM contents in pristine rivers, from Álvarez-Vázquez *et al.* (2016; 2017b).

clay particles, given that Al is usually more abundant in fines (Birch, 2020). The retention and enrichment of Fe might be driven by two possible processes forming coatings over sand surfaces: (i) trapped in Fe-oxyhydroxides (Tessier *et al.*, 1985) or/and (ii) stabilized by adsorption over surfaces in the form of organic matter-Fe complexes, an ordinary and significant process of Fe stabilization e.g. in soils (Chen *et al.*, 2014); being very immature sediments in oxygenic conditions, Fe is unexpected to be affected by post-depositional migrations. Except Cu in sample M05 (factor 0.9), the contents of trace elements were generally higher in the fine fraction, when compared with the < 2 mm fraction. This is: Cu was 1.6 times higher in the fine fraction of M05, Pb enrichment was 3.2 and 1.9 times higher in M02 and M05 respectively, and Zn contents were 11.9 times (in M02) and 3.4 times (in M05). This fact supports the hypothesis that the aforementioned hidden factor contributing to the variability of Cu, Pb and Zn could represent contamination. However, the metal-Fe ratios are similar between fractions, thus more data is needed to asseverate a contamination state.

These results point to a higher accumulation of trace metals as more abundant is the fine fraction, and this enrichment could be related with the behaviour of Fe. Trace elements can be stabilised by organic matter, trapping trace elements in Fe-oxyhydroxides or by the formation of ternary complexes over the Fe-oxyhydroxides (Tessier *et al.*, 1985). Consequently, Fe and trace elements can be enriched in the fine fraction by common sinking processes in quiet water masses like lakes. During the wet season the area is subjected to turbulent waters, but in summer the flow is low and, as observed in Fig. 5, the potholes are dry (losing water by evaporation) or flooded by quiet water. Possible processes are the adsorption to hydrous oxides of Fe, complexation with suspended particulate matter (particularly organic) and the uptake by phytoplankton (Borg, 1995). Note that the studied river reach is in the tail of a dam (commonly flooded by the reservoir waters). Reservoirs

possess a high capacity to trap both particulate and dissolved matter transported by rivers (Álvarez-Vázquez *et al.*, 2017). The fine fraction might be detecting some degree of contamination by Cu, Pb and Zn (Tables 2 and 3). This is particularly clear in the fine fraction of the sample M02, where the possible contamination is undetectable in the coarser <2 mm fraction.

5. Conclusion

Between the great diversity of the fluvial potholes, some of them present capacity to trap sediments. As result from this exploratory study, the characterization of the potholes as sediment traps need to consider their morphological configuration because it determines the possibility to store sediments. The position of the potholes regarding the bedrock channel also represents an important factor. In the studied site, the potholes that present conditions as sediment traps are located in the central and lateral sectors of the bedrock channel. They have a maximum vertical depth from 25 cm to 1 m, and preserve (totally or partially) their walls. The sediments trapped by these fluvial potholes are considered as representative concerning current dynamics in a small bedrock river.

The analysis of the mineralogy and the contents of major and trace elements from fluvial potholes reveals they are principally composed of a coarse-medium texture of sand-size and upward. The results indicated that the <2 mm fraction of the sediments is, as expected, reflecting the mineralogy of the source rock. Trace elements provided more information than major constituents did. While major constituents are related with the feldspar microcline, trace elements form three groups: a first one containing Ni related to albite and muscovite; a second containing Cr and linked to the quartz of sand; and a third linked to the microcline including Cu, Pb, and Zn. These last three elements reveal some hidden factor that could be related with some anthropogenic source of contamina-

tion. The fine fraction pointed to offer a more significant potential to detect contamination, which could be diluted in the sandy fraction of sediments. It is recommended to adapt the collection of samples to the requirements of the analytical technique because of the scarcity of fine particles in this type of systems. Expert based knowledge and on-site evaluation of the sediments is critical, e.g. to collect enough quantity of the rough sample for further analyses, considering that, the common abundance of the fine fraction may be below a 1% of the total.

The sediments trapped by fluvial potholes, with prevalence of the sand fraction, can be suitable to be used as environmental indicators of small bedrock rivers, even the statistical analysis of the less sensitive <2 mm fraction can be indicating the influence of any other factors, not only the mineral composition of sediments, in the contents of Cu, Pb and Zn. However, some questions should be boarded in future works. The fine fraction of sediments (<0.063 mm) concentrates common contaminants like Cu, Pb, and Zn, but this fraction is scarce in bedrock rivers; in consequence, in the study of bulk sediments the contamination might be obscured by dilution in the abundance of sandy quartz. Can the fine fraction be more suitable to detect and trace contamination? Fine sediments may have their origin in the weathering of parental rocks, but also in coatings and biofilms that have been detached in the drying-sieving process of the sample; as observed in the samples M02 and M05 the genesis of the fine fraction concentrates common contaminant elements. Like so, the question relies in the most adequate procedure to estimate background values and the selection of (e.g.) sample fractions or an appropriate reference element. Sediments trapped by potholes showed potential to be used as environmental indicators, but only after a careful selection of samples to get enough fine sediment to perform analysis, because this fraction seems to provide a better capacity to detect contamination. Forthcoming works will relay in the exploration of the sediment composition, de-

veloping procedures to set background values to determine contamination extent. This will allow detecting contamination hot-spots and critical areas of actuation, to provide valuable information for policy making and environmental management.

Acknowledgment

This research was partially financed by the project 'State of Geomorphological Heritage within the Thermal Surroundings of Ourense', reference INOU15-02, funded by the Vicerectorado do Campus de Ourense (University of Vigo) and the Diputación de Ourense. M.A. Álvarez-Vázquez is supported by the Xunta de Galicia through the postdoctoral grant #ED481B-2019-066.

References

- Alexander, H.S. (1932). Pothole erosion. *Journal of Geology*, 40, 305-337. <https://doi.org/10.1086/623954>
- Álvarez-Iglesias, P., Andrade, A., Rey, D., Quintana, B., Bernabéu, A., López-Pérez, A., Rubio, B. (2020). Assessment and timing of the anthropogenic imprint and fisheries richness in marine sediments from Ría de Muros (NW Iberian Peninsula). *Quaternary International*, 566-567, 337-356. <https://doi.org/10.1016/j.quaint.2020.05.005>
- Álvarez-Vázquez, M.A., De Uña-Álvarez, E. (2015). Recursos Geomorfológicos: Evolución Morfológica de las Marmitas de Erosión en el Miño Medio. *Actas do VII Simpósio Ibérico sobre a Bacia Hidrográfica do Rio Minho*. Câmara Municipal de Vila Nova de Cerveira, Portugal, 1-5.
- Álvarez-Vázquez, M.A., De Uña-Álvarez, E. (2017). Growth of sculpted forms in bedrock channels (Miño River, northwest Spain). *Current Science*, 112 (5), 996-1002. <https://doi.org/10.18520/cs/v112/i05/996-1002>
- Álvarez-Vázquez, M.A., Bendicho, C., Prego, R. (2014). Ultrasonic slurry sampling combined with total reflection X-ray spectrometry for multi-elemental analysis of coastal sediments in a ria system. *Microchemical Journal*, 112, 172-180. <https://doi.org/10.1016/j.microc.2013.09.026>

- Álvarez-Vázquez, M.A., Prego, R., Ospina-Álvarez, N., Caetano, M., Bernardez, P., Doval, M., Filgueiras, A.V., Vale, C. (2016). Anthropogenic changes in the fluxes to estuaries: Wastewater discharges compared with river loads in small rivers. *Estuarine, Coastal and Shelf Science*, 179, 112-123. <https://doi.org/10.1016/j.ecss.2015.08.022>
- Álvarez-Vázquez, M.A., Prego, R., Caetano, M., De Uña-Álvarez, E., Doval, M., Calvo, S., Vale, C. (2017). Contributions of trace elements to the sea by small uncontaminated rivers: Effects of a water reservoir and a wastewater treatment plant. *Chemosphere*, 178, 173-186. <https://doi.org/10.1016/j.chemosphere.2017.03.053>
- Barrera Morate, J.L., González Lodeiro, F., Marquínez García, J., Martín Parra, L.M., Martínez Catalán, J.R., Pablo Maciá, J.G. de. (1989). *Memoria del mapa geológico de España, Escala 1:200.000, Ourense/Verín*. Instituto Tecnológico GeoMinero de España, Madrid, 284 pp.
- Biggs, J., Von Fumetti, S., Kelly-Quinn, M. (2017). The importance of small waterbodies for biodiversity and ecosystem services: Implications for policy makers. *Hydrobiologia*, 793 (1), 3-39. <https://doi.org/10.1007/s10750-016-3007-0>
- Birch, G. (2020). An assessment of aluminum and iron in normalisation and enrichment procedures for environmental assessment of marine sediment. *Science of the Total Environment*, 727, 138123. <https://doi.org/10.1016/j.scitotenv.2020.138123>
- Birch, G., Lee, J. (2020). The use of sedimentary metal data in predictive modelling of estuarine contamination, assessment of environmental condition and pollutant source identification (Narrabeen lagoon, Sydney, Australia). *Environmental Science and Pollution Research*, 27, 43685-43699. <https://doi.org/10.1007/s11356-020-10279-0>
- Borg, H. (1995). Trace elements in lakes. In: B. Salbu and E. Steinnes (Eds.), *Trace elements in natural waters*. CRC Press, 177-201.
- Brunhes, J. (1899). Sur les marmites des îlots granitiques de la cataracte d'Assouan (Haute-Egypte). *Compte Rendus de l'Académie des Sciences*, 129, 345-357.
- Capdevila, R., Floor, P. (1970). Les different types de granites hercyniens et leur distribution dans le nord de l'Espagne. *Boletín Geológico y Minero*, LXXXI-II-III, 215-225.
- CEDEX. (2004). Directiva 2000/60/CE, Análisis de las características de las demarcaciones, Caracterización de los tipos de ríos y lagos. *Centro de Estudios y de Experimentación de Obras Públicas*, Madrid, 100 pp.
- Chen, C., Dynes, J.J., Wang, J., Sparks, D.L. (2014). Properties of Fe-organic matter associations via coprecipitation versus adsorption. *Environmental Science & Technology*, 48 (23), 13751-13759. <https://doi.org/10.1021/es503669u>
- CHMS. (2020). Documentos de planificación 2015-2021. *Confederación Hidrográfica Miño-Sil*. https://www.chminosil.es/images/reciente/Documentos_%20iniciales_MINO_SIL_V_DEF.pdf [Accessed 17 February 2020]
- Das, B.C. (2018). Development of Streambed Potholes and the Role of Grinding Stones. *Journal of Environmental Geography*, 11 (1-2), 9-16. <https://doi.org/10.2478/jengeo-2018-0002>
- De Uña-Álvarez, E. (2001). El clima. In: A. *Precedo Ledo and J. Sancho Comíns (Dir.)*, *Atlas de Galicia (I) Medio natural*. Xunta de Galicia, Santiago de Compostela, 137-155.
- De Uña-Álvarez, E., Vidal-Romaní, J.R., Rodríguez Martínez-Conde, R. (2009). Erosive forms in river systems. In: *Advances in Studies on Desertification (A. Romero, F. Belmonte, F. Alonso, and F. López, eds.)*. Editum, Murcia, 465-468.
- Dumas, C., Ludwig, W., Aubert, D., Eyrolle, F., Raimbault, P., Gueneugues, A., Sotin, D. (2015). Riverine transfer of anthropogenic and natural trace metals to the Gulf of Lions (NW Mediterranean Sea). *Applied Geochemistry*, 58, 14-25. <https://doi.org/10.1016/j.apgeochem.2015.02.017>
- Dupré, B., Gaillardet, J., Rousseau, D., Allègre, C.J. (1996). Major and trace elements of river-borne material: The Congo Basin. *Geochimica et Cosmochimica Acta*, 60(8), 1301-1321. [https://doi.org/10.1016/0016-7037\(96\)00043-9](https://doi.org/10.1016/0016-7037(96)00043-9)
- Elznicová, J., Grygar, M.T., Popelka, J., Sikora, M., Novák, P., Hošek, M. (2019). Threat of Pollution Hotspots Reworking in River Systems: Case Study of the Ploučnice River (Czech Republic). *ISPRS International Journal of Geo-Information*, 8 (1), 37. <https://doi.org/10.3390/ijgi8010037>
- Elston, E.D. (1917a). Potholes: their variety, origin and significance (I). *The Scientific Monthly*, V, 554-567.
- Elston, E.D. (1917b). Potholes: their variety, origin and significance (II). *The Scientific Monthly*, VI, 37-51.

- Falkenmark, M. (1997). Society's interaction with the water cycle: a conceptual framework for a more holistic approach. *Hydrological Sciences Journal*, 42 (4), 451-466. <https://doi.org/10.1080/02626669709492046>
- Fryirs, K.A., Brierley, G.J. (2012). *Geomorphic analysis of river systems: An approach to reading the landscape*. Wiley-Blackwell, Chichester, 360 pp. <https://doi.org/10.1002/9781118305454>
- Gaillardet, J, Dupré, B., Viers, J. (2003). Trace Elements in River Waters. In: *J.I. Drever (Ed.), Treatise on Geochemistry*, volume 5. Elsevier Science, San Diego, 225-272. <https://doi.org/10.1016/B0-08-043751-6/05165-3>
- Geiki, A. (1865). *The Scenery of Scotland*. Macmillan, London, 360 pp.
- Guinoiseau, D., Bouchez, J., Gélabert, A., Louvat, P., Filizola, N., Benedetti, M.F. (2016). The geochemical filter of large river confluences. *Chemical Geology*, 441, 191-203. <https://doi.org/10.1016/j.chemgeo.2016.08.009>
- Grygar, T.M., Elznicová, J., Lelková, T., Kiss, T., Balogh, M., Strnad, L., Navrátil, T. (2017). Sedimentary archive of contamination in the confined channel of the Ohře River, Czech Republic. *Journal of Soils and Sediments*, 17, 2596-2609. <https://doi.org/10.1007/s11368-017-1664-x>
- Håkanson, L. (2006). A dynamic model for suspended particulate matter (SPM) in rivers. *Global Ecology and Biogeography*, 15, 93-107. <https://doi.org/10.1111/j.1466-822X.2006.00196.x>
- Håkanson, L., Mikrenska, M., Petrov, K., Foster, I. (2005). Suspended particulate matter (SPM) in rivers: Empirical data and models. *Ecological Modelling*, 183 (2-3), 251-267. <https://doi.org/10.1016/j.ecolmodel.2004.07.030>
- Helios Rybicka, E., Adamiec, E., Aleksander-Kwaterczak, U. (2005). Distribution of trace metals in the Odra River system: Water-suspended matter-sediments. *Limnologica*, 35 (3), 185-198. <https://doi.org/10.1016/j.limno.2005.04.002>
- Hodge, R.A., Hoey, T.B., Sklar, L.S. (2011). Bed load transport in bedrock rivers: The role of sediment cover in grain entrainment, translation, and deposition. *Journal of Geophysical Research Atmospheres*, 116, F04028. <https://doi.org/10.1029/2011JF002032>
- Ives, R.L. (1948). Plunge pools, potholes and related features. *Rocks and Minerals*, 23, 3-10.
- James, L.A., Marcus, W.A. (2006). The human role in changing fluvial systems: Retrospect, inventory and prospect. *Geomorphology*, 79 (3-4), 152-171. <https://doi.org/10.1016/j.geomorph.2006.06.017>
- Ji, S., Zeng, W., Li, L., Ma, Q., Feng, J. (2019). Geometrical characterization of stream potholes in sandstone from the Sunxi River (Chongqing, China) and implications for the development of bedrock channels. *Journal of Asian Earth Sciences*, 173, 374-385. <https://doi.org/10.1016/j.jseaes.2019.01.037>
- Kanhaiya, S., Singh, S., Singh, C. K., Srivastava, V. K. (2019). Pothole: a unique geomorphological feature from the bedrocks of Ghaghghar River, Son valley, India. *Geology, Ecology, and Landscapes*. <https://doi.org/10.1080/24749508.2018.1558018>
- Kronvang, B., Wendland, F., Kovar, K., Fraters, D. (2020). Land Use and Water Quality. *Water*, 12, 2412. <https://doi.org/10.3390/w12092412>
- Lorenc, M.W., Muñoz Barco, P., Saavedra Alonso, J. (1994). The evolution of potholes in granite bedrock, W Spain. *Catena*, 22, 265-274. [https://doi.org/10.1016/0341-8162\(94\)90037-X](https://doi.org/10.1016/0341-8162(94)90037-X)
- Lorenc, M.W., Muñoz Barco, P., Saavedra Alonso, J. (1995). Marmitas de gigante en el valle del río Jerte como ejemplo de erosión fluvial intensiva por remolinos e influencia tectónica en su distribución y morfología. *Cuaternario y Geomorfología*, 9 (1/2), 17-26.
- Martín-González, F. (2009). Cenozoic tectonic activity in a Variscan basement: Evidence from geomorphological markers and structural mapping (NW Iberian Massif). *Geomorphology*, 107, 210-225. <https://doi.org/10.1016/j.geomorph.2008.12.008>
- Messerli, B., Grosjean, M., Hofer, T., Nuñez, L., Pfister C. (2000). From nature-dominated to human-dominated environmental changes. *Quaternary Science Reviews*, 19 (1-5), 459-479. [https://doi.org/10.1016/S0277-3791\(99\)00075-X](https://doi.org/10.1016/S0277-3791(99)00075-X)
- Meybeck, M., Helmer, R. (1989). The quality of rivers: from pristine stage to global pollution. *Global and Planetary Change*, 1 (4), 283-309. [https://doi.org/10.1016/0921-8181\(89\)90007-6](https://doi.org/10.1016/0921-8181(89)90007-6)
- Moatar, F., Abbott, B.W., Minaudo, C., Curie, F., Pinay, G. (2017). Elemental properties, hydrology, and biology interact to shape concentration-discharge curves for carbon, nutrients, sediment, and major ions. *Water Resources Research*, 53, 1270-1287. <https://doi.org/10.1002/2016WR019635>
- Nemec, W., Lorenc, M.W., Saavedra Alonso, J. (1982). Potholed granite terrace in the río Salor valley, western Spain: a study of bedrock erosion by floods. *Tecniterrae*, 50, 6-21.

- Ortega Becerril, J.A., Durán Valseiro, J.J. (Eds.) (2010). *Patrimonio geológico: los ríos en roca de la Península Ibérica*. Instituto Geológico y Minero de España, Madrid, 497 pp.
- Ortega, J.A., Gómez-Heras, M., Pérez-López, R., Wohl, E.E. (2014). Multiscale structural and lithologic controls in the development of stream potholes on granite bedrock rivers. *Geomorphology*, 204, 588-598. <https://doi.org/10.1016/j.geomorph.2013.09.005>
- Ortega-Becerril J. A., Gómez-Heras, M., Fort, R., Wohl, E.E. (2017). How does anisotropy in bedrock river granitic outcrops influence pothole genesis and development? *Earth Surface Processes and Landforms*, 42 (6), 956-968. <https://doi.org/10.1002/esp.4054>
- Rice, K.C. (1999). Trace-Element Concentrations in Streambed Sediment Across the Conterminous United States. *Environmental Science and Technology*, 33 (15), 2499–2504. <https://doi.org/10.1021/es990052s>
- Richardson, K., Carling, P.A. (2005). *A Typology of Sculpted Forms in Open Bedrock Channels*. *Geological Society of America*, Special paper 392, Boulder, Colorado, 108 pp. <https://doi.org/10.1130/0-8137-2392-2.1>
- Silva, D. C., Bellato, C. R., Marques Neto, J. O., Fontes, M.P. F. (2018). Trace elements in river waters and sediments before and after a mining dam breach (Bento Rodrigues, Brazil). *Química Nova*, 41 (8), 857-866. <https://doi.org/10.21577/0100-4042.20170252>
- Springer, G.S., Tooth, S., Wohl, E.E. (2006). Theoretical modeling of stream potholes based upon empirical observations from the Orange River, Republic of South Africa. *Geomorphology*, 82 (1-2), 160-176. <https://doi.org/10.1016/j.geomorph.2005.09.023>
- Tessier, A., Rapin, F., Carignan, R. (1985). Trace metals in oxic lake sediments: Possible adsorption onto iron oxyhydroxides. *Geochimica et Cosmochimica Acta*, 49 (1), 183-194. [https://doi.org/10.1016/0016-7037\(85\)90203-0](https://doi.org/10.1016/0016-7037(85)90203-0)
- Tinkler, J. K., Wohl, E. E. (Eds.) (1998). *Rivers over Rock: Fluvial Processes in Bedrock Channels*. American Geophysical Union, Washington D.C., 323 pp. <https://doi.org/10.1029/GM107>
- Tschang, H. (1957). Potholes in the river beds of North Taiwan. *Erdkunde*, XI(4), 292-303. <https://doi.org/10.3112/erdkunde.1957.04.05>
- Turowski, J.M. (2020) Mass balance, grade, and adjustment timescales in bedrock channels. *Earth Surface Dynamics*, 8, 103–122. <https://doi.org/10.5194/esurf-8-103-2020>
- Uddin, M.J., Jeong, Y.K. (2021). Urban river pollution in Bangladesh during last 40 years: potential public health and ecological risk, present policy, and future prospects toward smart water management. *Heliyon*, 7 (2), E06107. <https://doi.org/10.1016/j.heliyon.2021.e06107>
- Udomsak, S., Choowong, N., Choowong, M., Vichai Chutakositkanon, V. (2021). Thousands of Potholes in the Mekong River and Giant Pedestal Rock from North-eastern Thailand: Introduction to a Future Geological Heritage Site. *Geoheritage*, 13 (5). <https://doi.org/10.1007/s12371-020-00524-w>
- Vegas, R. (2010). La continuación de la Cordillera Cantabro-Pirenaica en el borde atlántico de la Península Ibérica. *Geogaceta*, 48, 179-181.
- Verstraeten, G. (2019). *Human Impact on Historical Fluvial Sediment Dynamics in Europe*. <https://www.oxfordbibliographies.com/view/document/obo-9780199363445/obo-9780199363445-0122.xml> [Accessed 15 December 2020]. <https://doi.org/10.1093/obo/9780199363445-0122>
- Vidal-Romaní, J.R., Martelli, A., Fernández-Mosquera, D., De Uña, E., Yepes, J. (2005). Galicia Region: Landforms and Morphological Evolution of Granitic Areas. *Sixth International Conference on Geomorphology*, Zaragoza, 36 pp.
- Vidal-Romaní, J.R., Vaqueiro, M., Sanjurjo, J. (2014). Granite Landforms in Galicia. In: F. Gutiérrez and M. Gutiérrez, *Landscapes and Landforms of Spain*. Springer, Dordrecht, 63-69. https://doi.org/10.1007/978-94-017-8628-7_4
- Viers, J., Dupré, B., Gaillardet, J. (2009). Chemical composition of suspended sediments in World Rivers: New insights from a new database. *Science of the Total Environment*, 407 (2), 853-868. <https://doi.org/10.1016/j.scitotenv.2008.09.053>
- Vital, H., Stattegger, K. (2000). Major and trace elements of stream sediments from the lowermost Amazon River. *Chemical Geology*, 168 (1-2), 151-168. [https://doi.org/10.1016/S0009-2541\(00\)00191-1](https://doi.org/10.1016/S0009-2541(00)00191-1)
- Viveen, W., Braucher, R., Bourlés, D., Schoorl, J., Veldkamp, A., Van Balen, R., Wallinga, J., Fernandez Mosquera, D., Vidal Romaní, J., Sanjurjo Sanchez, J. (2012). A 0.65 Ma chronology and incision rate assessment of the NW Iberian Miño River terraces based on ¹⁰Be and luminescence dating. *Global and Planetary Change*, 94-95, 82 - 100. <https://doi.org/10.1016/j.gloplacha.2012.07.001>

- Viveen, W., Schoorl, J.M., Veldkamp, A., van Balen, R.T. (2014). Modelling the impact of regional uplift and local tectonics on fluvial terrace preservation. *Geomorphology*, 210, 119-135. <https://doi.org/10.1016/j.geomorph.2013.12.026>
- Wentworth, C.K. (1944). Potholes, pits and pans: subaerial and marine. *Journal of Geology*, 52, 117-130. <https://doi.org/10.1086/625198>
- Whipple, K.X., Hancock, G.S., Anderson, R.S. (2010). River incision into bedrock: Mechanics and relative efficacy of plucking, abrasion, and cavitation. *Geological Society of America Bulletin*, 112 (3), 490-503. [https://doi.org/10.1130/0016-7606\(2000\)112<490:RIIBMA>2.0.CO;2](https://doi.org/10.1130/0016-7606(2000)112<490:RIIBMA>2.0.CO;2)
- Wilkinson, W. B., Leeks, G.J.L., Morris, A., Walling, D.E. (1997). Rivers and coastal research in the Land Ocean Interaction Study. *Science of the Total Environment*, 194-195, 5-14. [https://doi.org/10.1016/S0048-9697\(96\)05350-8](https://doi.org/10.1016/S0048-9697(96)05350-8)
- Wohl, E.E. (2015). Particle dynamics: The continuum of bedrock to alluvial river segments. *Geomorphology*, 241, 192-208. <https://doi.org/10.1016/j.geomorph.2015.04.014>
- Wohl, E.E. (2020). *Rivers in the Landscape*. Wiley, Hoboken, Second edition, 500 pp. <https://doi.org/10.1002/9781119535409>
- Wohl, E.E., Merritt, D.M. (2001). Bedrock channel morphology. *Geological Society of America Bulletin*, 113 (9), 1205-1212. [https://doi.org/10.1130/0016-7606\(2001\)113<1205:BCM>2.0.CO;2](https://doi.org/10.1130/0016-7606(2001)113<1205:BCM>2.0.CO;2)
- Xu, F., Liu, Z., Cao, Y., Qiu, L., Feng, J., Xu, F., Tian, X. (2017). Assessment of heavy metal contamination in urban river sediments in the Jiaozhou Bay catchment, Qingdao, China. *Catena*, 150, 9-16. <https://doi.org/10.1016/j.catena.2016.11.004>
- Yepes Temiño, J. (2002). Geomorfología de un sector comprendido entre las provincias de Lugo y Ourense. *Laboratorio Xeolóxico de Laxe, Serie Nova Terra, A Coruña*, 273 pp.

Recibido el 21 de abril de 2021
Aceptado el 25 de mayo de 2021

